Journal of Low Temperature Physics, Vol. 129, Nos. 3/4, November 2002 (© 2002)

Slow Diffusion of Molecular Hydrogen in Zeolite 13X

J. DeWall,[1,*] R. M. Dimeo,[2] and P. E. Sokol[1]

[1] *Department of Physics, The Pennsylvania State University, University Park, Pennsylvania 16802*
E-mail: paul@sokol.phys.psu.edu
[2] *NIST Center for Neutron Research, National Institute of Standards and Technology, 100 Bureau Drive, Stop 8562, Gaithersburg, Maryland 20899*

(Received June 13, 2002; revised July 27, 2002)

High-resolution quasi-elastic neutron scattering measurements have been performed on molecular hydrogen in zeolite 13X. Previous NMR measurements suggested that the freezing temperature is suppressed from 14 K down to 8 K. In contrast, previous intermediate resolution quasi-elastic neutron scattering studies suggested freezing occurred between 25 and 35 K. Unfortunately, the limited instrumental resolution available in the previous quasi-elastic neutron scattering study was not sufficient to show this point definitively. We report new quasi-elastic neutron scattering measurements with very high resolution that show no evidence of mobile hydrogen below 25 K, which is well above the bulk liquid-solid transition temperature for hydrogen. A quasi-elastic component appears between 25 and 30 K indicating the presence of mobile H_2. However, the width and momentum dependence of the quasi-elastic scattering are much different than would be expected for the diffusive motion of liquid hydrogen in this temperature range. Instead, we find that a slow diffusive component representing jumps between well-defined sites appears first at low temperatures. As the temperature is raised, a faster liquid like diffusive component appears.

1. INTRODUCTION

Superfluids are quite rare in nature, with ^{4}He and ^{3}He at low temperature being the only naturally occurring examples.[1] The extraordinary interest generated by the production of atomic Bose condensates[2] highlights the interest in studying new manifestations of superfluids. Thus, the prediction that molecular hydrogen may become superfluid at around 6 K

* Current Address: Navigation Research & Development Center, Penn State Applied, Research Lab, Warminster, Pennsylvania 18974.

0022-2291/02/1100-0171/0 © 2002 Plenum Publishing Corporation

by Ginzburg and Sobyanin[3] generated a great deal of theoretical and experimental interest. While this estimate, based on the ideal gas result, is overly optimistic[4] since it is based on a simple analytical result, it does provide a useful order of magnitude for the transition. More realistic estimates[5] yield a transition temperature in the range of 2–3 K. Unfortunately, nature has conspired to keep superfluids a rarity—the liquid-solid transition in bulk hydrogen[6] occurs well above the Bose condensation temperature, preempting any possible superfluid phase at lower temperatures in the bulk.

Suppressing the solid phase of hydrogen, by supercooling the liquid below its normal freezing temperature of 13.8 K, offers the only possibility for observing Bose condensation and much work[5, 7, 8] has focused on this possibility. One possible approach, confinement in restricted geometries, has attracted considerable interest since many systems exhibit a suppressed freezing transition.[9] The suppression of the freezing temperature arises from the competition between volume and surface effects in the nucleation of the solid phase and is inversely proportional to the pore size. Studies of hydrogen in Vycor,[8, 10–13] a porous glass with 70 Å diameter pores, observed a suppression of the freezing temperature by as much as a few Kelvin. Thus, confinement in small enough pores, on the order of 20 Å, could move the freezing temperature below the Bose condensation temperature allowing a new superfluid to be stabilized.

Zeolites are crystalline materials with well-defined pores on the order of 10 Å interconnected by channels in a crystalline three dimensional structure. As such, they[8, 14] are a natural step in the possible realization of superfluid hydrogen. NMR studies[8, 13] of H_2 in zeolite 13X[15] have reported a suppression of the liquid-solid freezing temperature to 8 K, approaching the Bose condensation temperature predicted by Ginzburg and Sobyanin. However, neutron diffraction studies[16] of D_2, an isotope of H_2, in zeolite 13X showed that the D_2 molecules are strongly absorbed in specific sites determined by the zeolite structure. Furthermore, the zeolite-D_2 interactions supercede D_2–D_2 interactions, which are necessary in the conventional idea of a solid phase. That is, the absorbed deuterium does not behave as a conventional solid phase. Instead, the D_2 atoms occupy well defined binding sites of the zeolite lattice and are simply a new component of the zeolite structure itself. Quasi elastic neutron scattering studies,[17] which probe the self diffusion of the hydrogen molecule, support the diffraction studies. They observed no diffusive motion below 35 K making it unlikely that a liquid phase exists at lower temperatures. Unfortunately, the instrumental resolution of the spectrometer used in those studies limited the minimum diffusivity measurable. Thus they were unable to definitely state that a liquid, or mobile, phase was absent below 35 K.

We report here studies of the low-frequency dynamics of H_2 absorbed in zeolite with quasi-elastic neutron scattering (QENS). QENS is ideally suited to observing the diffusive behavior of the molecules. The energy width of the quasi-elastic scattering is directly related to the diffusion constant and the dependence of the width on momentum transfer provides information on the type of diffusion (i.e., free diffusion, finite range hopping, random length hopping, etc.). Zeolite 13X was used as a host for the hydrogen, as in the previous studies, and the measurements were carried out using the High Flux Backscattering Spectrometer (HFBS) at the NIST Center for Neutron Research (NCNR) in Gaithersburg, Maryland.[18] The excellent energy resolution of this spectrometer addresses the limitations of the previous study and allows extremely slow molecular motions to be observed.

Our measurements are consistent with the previous neutron diffraction and QENS studies. They show no evidence of mobile hydrogen below 25 K, which is well above the bulk liquid-solid transition temperature for hydrogen. A quasi-elastic component appears in the scattering between 25 and 30 K indicating the presence of mobile H_2. However, the width and momentum dependence of the quasi-elastic scattering are much different than would be expected for the diffusive motion of liquid hydrogen in this temperature range. Instead, we find that a slow diffusive component representing jumps between well-defined sites appears first at low temperatures. As the temperature is raised a faster liquid like diffusive component appears which is consistent with the variable range hopping observed in previous measurements.

2. EXPERIMENTAL DETAILS

The High Flux Backscattering Spectrometer[18] (HFBS) operates with a fixed final beam energy of 2.08 meV, determined by the d-spacing of the (111) lattice planes of the silicon analyzer. The spherically focusing analyzer system, composed of a large array of Si (111) wafers subtending 20% of a solid sphere, backscatters the neutrons into 16 independent detectors located from about 15 to 120° with respect to the incident beam. The incident beam is focused to 2.08 meV with a phase space transform chopper before being varied in energy with a Doppler monochromator and sent through the sample. The Doppler monochromator consists of a silicon monochromator connected to a Doppler drive which varies the incident beam's energy by ± 26 μeV about 2.08 meV. The HFBS, with a resolution of ~ 1 μeV, is designed to provide ultra-high resolution measurements of low-frequency dynamic systems. By comparison, previous QENS studies of this system have been carried out with resolutions of 75 μeV.

The zeolite used in this study was commercially available 13X[15] (1) crushed into a powder. Zeolite 13X consists of a rigid backbone composed of silicon, aluminum, and oxygen with a Si/Al ratio of 1.24. A zeolite 13X crystal has a face centered cubic structure (space group Fd3) with unit cell dimensions of 25 Å per side.[19] The structure consists of approximately 13 Å diameter cavities connected by channels with diameters of approximately 10 Å. The powdered zeolite crystals were heated to 500 K in vacuum for several hours to remove impurities, primarily water, and were then confined to the geometry of a thin slab whose normal was oriented at 45° with respect to the incident beam. The cell was then mounted in a standard "orange" cryostat to allow measurements at low temperatures.

Normal hydrogen gas (n-H_2) was introduced to the sample cell at 60 K and 1 bar. Previous measurements[16,17] have shown that loading at this pressure is sufficient to completely fill the first monolayer. The n-H_2 was then pumped away and the cell temperature was decreased to 20 K for the first measurement. Measurements were taken at temperatures ranging from 5 to 70 K which were kept within 0.1 degrees of the desired values during the course of each measurement. The cell was vacated of hydrogen as the temperature was raised to 200 K. The empty zeolite sample was then cooled to 5 K and data was taken against which the measurements in the presence of H_2 would later be compared. The empty zeolite data provided a completely elastic scattering peak from which the instrumental resolution of about 1 μeV (FWHM of the peak) could be determined.

The raw scattering data was converted to the dynamic scattering function, $S(Q, E)$ using standard techniques. Ortho-para conversion of the n-H_2 was not taken into account in the analysis. The HFBS spectrometer utilizes a Doppler monocromator to select the incident energy. This monochromator, which operates at ~ 10 Hz, allows a complete measurement of the scattering to be carried out every 0.1 s. Subsequent measurements increase the statistics of the measurements. This time scale is sufficiently fast that ortho-para conversion, which occurs on a much slower time scale, will not change the shape of the quasi-elastic scattering from which the diffusion constant is extracted. In addition, Rall *et al.*[20] have shown that the ortho-para conversion of H_2 confined in zeolite 13X is significantly slower than in the bulk for the first 500 h of confinement. Thus, during the time scale of our measurement (~ 100 h) the ortho-para concentrations would have changed by only $\sim 15\%$.

[1] Manufacturers are identified in order to provide complete identification of experimental conditions, and such identification is not intended as a recommendation or endorsement by NIST.

3. RESULTS AND ANALYSIS

Figure 1 depicts the observed scattering, with an emphasis on the broadening of the elastic peak as a function of temperature. As can be seen, no quasi-elastic scattering is present for temperatures between 5 and 25 K. The peak at 20 K is identical to the resolution of the instrument indicating that no diffusive motion is occurring. As the temperature is increased quasi-elastic scattering from the hydrogen appears indicating diffusive motion of the hydrogen on the timescale of about 0.4 ns. As the temperature is increased the quasi-elastic scattering broadens indicating an increase in the diffusion rate. Finally, at 70 K, the scattering becomes too broad for the dynamic range of the instrument and shows up only as an apparent increase in the background level.

The scattering shown in Fig. 1 can be characterized by an elastic peak and a quasi-elastic-scattering component. The elastic scattering is a delta-function in energy and represents immobile hydrogen and the scattering from the confining zeolite. The quasi-elastic scattering is broader than the narrow elastic peak and is readily visible at intermediate temperatures. At higher temperatures the scattering becomes sufficiently broad that it appears as an increase in the background level of the measurement. We have fit the scattering using a three component model scattering function

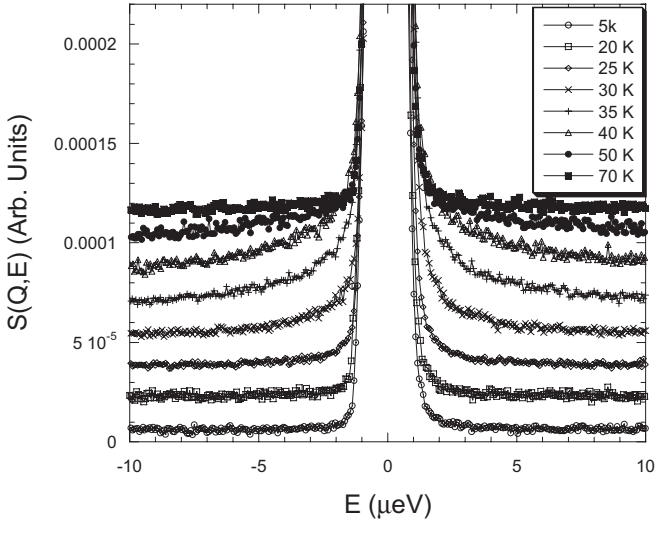

Fig. 1. The scattering from H_2 in zeolite at several temperatures between 5 and 70 K. The temperatures of the measurement are identified in the figure legend. The elastic scattering around $E = 0$ has been truncated to allow the quasi-elastic to more easily be seen.

—a narrow Gaussian component representing the elastic scattering, a Lorentzian component representing the quasi-elastic scattering, and a linear term to account for the background level. This model scattering function is convolved with the experimental resolution, determined from the low temperature empty cell measurements, and fit to the data using standard fitting procedures. A typical fit to the data is shown in Fig. 2. As can be seen this model provides excellent agreement with the experimental results. Similar quality fits are obtained at each detector angle and at each temperature.

The momentum transfer (Q) dependence of the width of the quasi-elastic scattering peak provides useful information not only on the diffusion constant but also on the diffusion mechanism. The Lorentzian FWHM for each detector is plotted versus Q for measurements at 40 K in Fig. 3. As can be seen the width increases rapidly at small Q and then oscillates about a fixed value at larger Q's. The results show this behavior for temperatures from 25 to 50 K. At 50 K the scattering is becoming very broad, compared to the dynamic range of the instrument, and the oscillations are less pronounced as shown in Fig. 4. Above 50 K the scattering becomes sufficiently broad, compared to the dynamic range of the instrument, that it is difficult to extract accurate parameters and we have not attempted to do so.

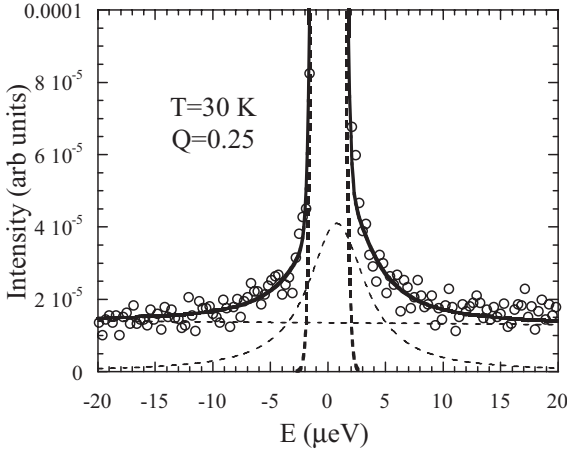

Fig. 2. Observed scattering at 30 K and $Q = 0.25\,\text{Å}^{-1}$. The solid line is a fit to the data of the model discussed in the text broadened by the measured instrumental resolution. The heavy dashed line shows the elastic component and the light dashed line shows the Lorentzian component. Both components have been broadened by the instrumental resolution.

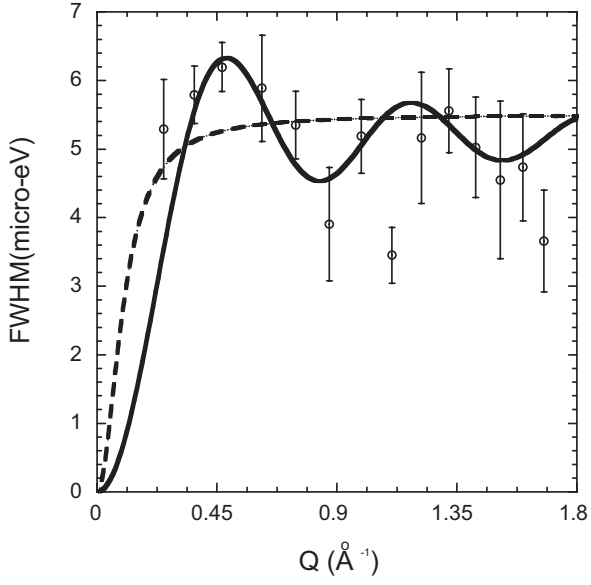

Fig. 3. The Lorentzian FWHM, extracted from fits of the model scattering to the data as a function of Q, at 40 K. The solid line is a fit of the Chudley–Elliot diffusion model. The dashed line is a fit of the Variable Jump Length diffusion model.

The behavior of the scattering widths for temperatures between 30 and 40 K as a function of momentum transfer was modeled using the Chudley–Elliot model of translational jump diffusion with a fixed jump length.[21] Although originally developed to explain diffusion in a liquid, the model can be applied to solid state systems as well.[22] For our purposes, since we used powdered zeolite, the jump diffusion model averaged over all space was used. In this model,

$$\Lambda(Q) = \frac{2 \cdot \hbar}{\tau}\left(1 - \frac{\sin Q\ell}{Q\ell}\right) = \frac{12 \cdot \hbar \cdot D_s}{\ell^2}\left(1 - \frac{\sin Q\ell}{Q\ell}\right),$$

where $\Lambda(Q)$ is the full width at half maximum of the Lorentzian, ℓ is the fixed jump length, τ is the residence time at any given site, and D_s is the self-diffusion constant.[22] Figure 3 shows the results of a fit of the Chudley–Elliot diffusion model to the 40 K scattering data. As can be seen this model reproduces the main features of the data and provides a relatively good fit at temperatures of 30, 35, and 40 K. The diffusion coefficient, D_s, and the jump length, ℓ, determined from the fitting parameters are listed in Table I.

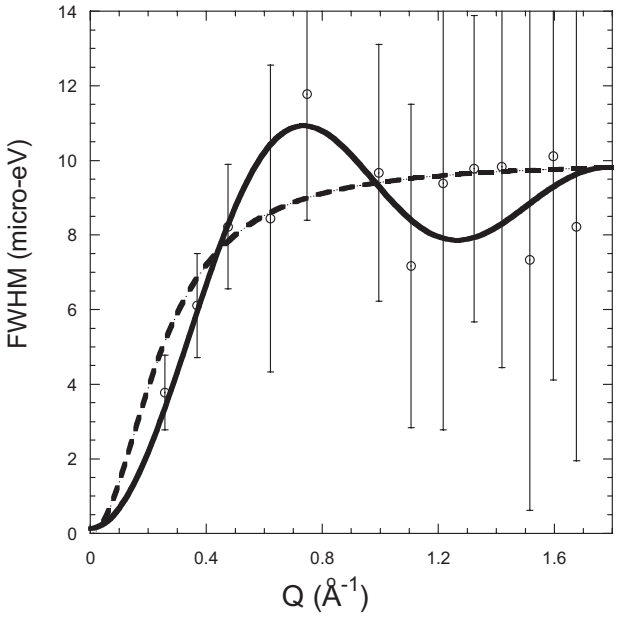

Fig. 4. The Lorentzian FWHM, extracted from fits of the model scattering to the data as a function of Q, at 50 K. The solid line is a fit of the Chudley–Elliot diffusion model. The dashed line is a fit of the Variable Jump Length diffusion model.

Table I

The Diffusion Coefficients and Jump Lengths Extracted from Fits to the Width as a Function of Momentum Transfer at Various Temperatures. The Column Labeled Model Refers to the Models Used to Determine These Parameters. The Chudley–Elliot (CE) Model and Variable Jump Length (VJL) Models Are Discussed in the Text

Temperature (K)	Model	Diffusion coefficient (10^{-10} m^2/s)	Jump length (Å)
30	CE	2.84 ± 0.40	8.63 ± 0.55
35	CE	3.10 ± 0.58	8.60 ± 0.74
40	CE	4.98 ± 0.70	8.86 ± 0.60
50	CE	3.9±2.0	6.2±1.3
	VJL	23±12	4.0±1.5

Previous studies of H_2 in zeolite by Fu, Trouw, and Sokol[17] observed quasi-elastic scattering at comparable temperatures (35–40 K). Their results could be modeled with a variable length jump diffusion model[23]

$$\Lambda(Q) = \frac{12 \cdot \hbar \cdot D_s}{\ell_0^2}\left(1 - \frac{1}{1 + Q^2\ell_0^2}\right),$$

where l_0 is a characteristic jump length. This model assumes a distribution of jump lengths

$$d(\ell) = \frac{\ell}{\ell_0^2} e^{-\ell/\ell_0}$$

rather than a single fixed jump length as in the Chudley–Elliot model. A fit of the 40 K data to the variable length jump model is also shown in Fig. 3. As can be seen this model does not qualitatively reproduce the observed Q dependence.

The 50 K data exhibits behavior that is qualitatively different from that at lower temperatures. Due to the broad width of the scattering, compared to the dynamic range of the instrument, the extracted widths have significantly larger experimental errors. At the same time, the oscillation of the width, which is quite evident at lower temperatures, is much less pronounced. Figure 4 shows a fit of both the Chudley–Elliot and the variable length jump models to the experimental results. The Chudley–Elliot model gives a slightly better statistical fit. However, both models provide an adequate description of the data due to the large experimental errors.

While the Chudley–Elliot model provides an adequate description of the 50 K results the diffusion constant that it yields exhibits unphysical behavior. As can be seen in Table I the diffusion constant from the Chudley–Elliot model decreases by 20% as the temperature is raised from 40 to 50 K. This is in contrast to our physical expectations and to the trend of the lower temperature data. The variable jump length model, in contrast, yields a diffusion constant that increases with temperature. In fact, the diffusion constant obtained from the variable jump length model is in good agreement with previous measurements. We believe that this indicates a change in the diffusion mechanism from a fixed length Chudley–Elliot type diffusion to a variable jump length diffusion between 40 and 50 K.

The diffusion coefficients obtained from the above fits, as well as the results obtained by Fu, Trouw, and Sokol,[17] are shown in Fig. 5. As can be seen both our results and the previous studies exhibit thermally activated behavior, $D = D_0 e^{-\Delta/kT}$. The previous studies extracted a thermal activation energy of $\Delta = 62 \pm 11$ K and a prefactor of $D_0 = (1.20 \pm 0.27) \times 10^{-8}$ m^2/s.

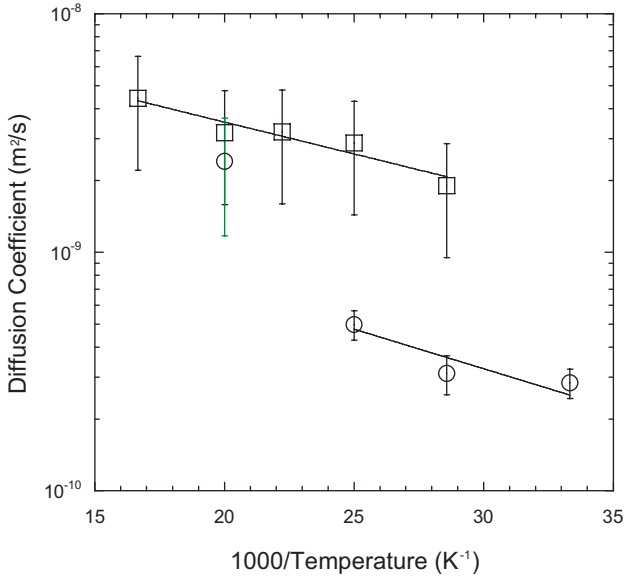

Fig. 5. The diffusion coefficients resulting from the Chudley–Elliot diffusion model are plotted as circles in a semi-log plot. The diffusion coefficients from the paper by Fu, Trouw, and Sokol[17] are shown as boxes. The solid lines represent logarithmic fits to the respective data. Our diffusion constant for the 50 K data (not included in the fit) shows a change in the diffusion mechanism from the lower temperatures.

Our result at 50 K is consistent with these measurements. At lower temperatures (30–40 K) we also observe temperature dependence consistent with a thermally activated behavior. However, due to the limited range of temperatures the behavior might also be consistent with other models for the temperature dependence. Assuming a thermally activated behavior we obtain $\Delta = 76 \pm 33$ K and $D_0 = (3.19 \pm 2.5) \times 10^{-9}$ m^2/s. The activation energy for these lower temperature measurements is, within the rather large experimental error, the same as for the higher temperature measurements. The prefactor, on the other hand, is nearly an order of magnitude smaller.

4. DISCUSSION

The fixed-length jump diffusion observed at lower temperatures (30, 35, and 40 K) can be understood in terms of the structure of the confining zeolite. The zeolite crystal structure, obtained from the measured atomic coordinates and space group,[19] is shown in Fig. 6. The segment shown in the figure is one of the many 13 Å diameter cavities, which comprise

zeolite, as seen through a channel. Neutron diffraction studies[16] showed that D_2 was strongly absorbed in two specific binding sites within the zeolite structure. Of the two sites, designated s1 and s2, s1 had a larger binding energy (~ 80 K) than s2 (~ 40 K). The diffraction studies did not, however, identify the crystallographic location of the binding sites.

Based upon the diffraction studies and the known structure of zeolite we have tentatively identified the crystallographic locations of the binding sites. We propose that the s1 binding site is located within the 13 Å cavity and has a multiplicity of four per cavity arranged in a tetrahedral manner and is shown in Fig. 6. The s2 binding site is located adjacent to the channel openings in the cage and is not shown in the figure. Although a complete structural determination of the sites s1 and s2 via Reitveld

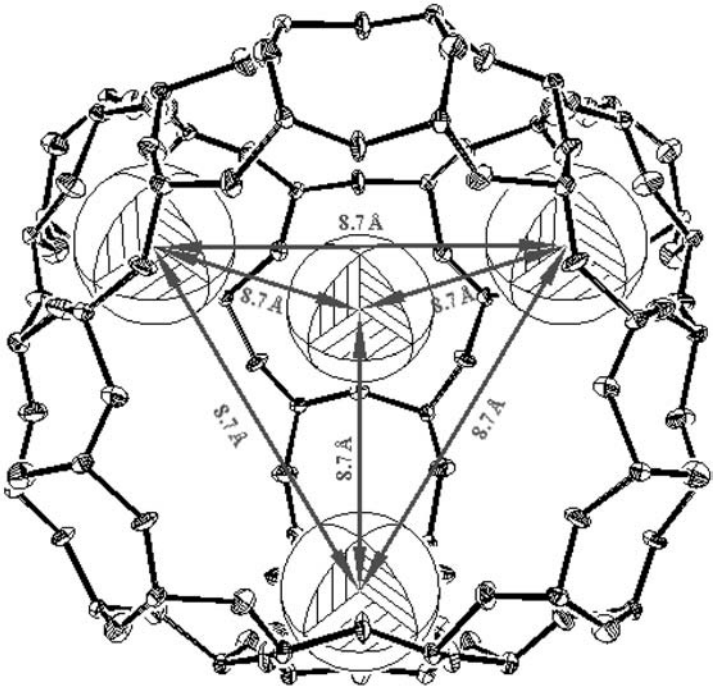

Fig. 6. A view of a single zeolite cage is shown as peering through a channel opening. These openings are located in a tetragonal manner about each cage. Each cage has four adjacent cages connected to these openings. The openings line up in such a way as to create channels that extend throughout the entire structure. The four sl binding sites per cage are also shown, located directly opposite the openings and 8.7 Å away from adjacent sites. The s2 binding sites are not shown in the interest of clarity of the figure. They are situated along the channels and number six per cage.

refinement[24–27] was not performed, the locations of the proposed s1 and s2 sites were correlated empirically by comparing the published diffraction patterns of D_2 in zeolite[28] to diffraction patterns generated with the Generalized Structure Analysis System (GSAS)[29]. The proposed binding sites give good agreement with the published diffraction patterns.

The s1 binding site shown in Fig. 6 has multiplicity of four per cavity arranged in a tetrahedral manner and separated by 8.7 Å. This corresponds well to the fixed jump length of $\ell = 8.70 \pm 0.37$ Å which we observe for our lower temperature measurements. Thus, we believe that the slow diffusion process we observe is jump diffusion between s1 sites. The diffraction studies also identified these sites as having the higher binding energy, which more likely corresponds to the relatively slow diffusion mechanism seen in this paper.

The diffusion constants shown in Fig. 5 show two distinct regimes, a slow diffusion between 30 and 40 K, and a more rapid diffusion above 35 K. In general, we would expect the previous measurements of Fu *et al.*,[17] with a resolution of 75 μeV, to observe only the rapid diffusion. The slow diffusion component, due to its much smaller width, would appear as part of the elastic peak. Likewise, in this measurement with its excellent energy resolution (~ 1 μeV) we would expect to see only the slow diffusion component. The rapid diffusion observed by Fu *et al.*, has a width on the order of 100 μeV which is much larger than the dynamic range of the instrument (± 26 μeV). We would not expect to observe quasi-elastic scattering associated with this rapid motion since the signal would not appear as a peak but simply as an increase in the background level.

We do, however, observe the rapid diffusion component in this measurement at the highest temperature studied. However, the parameters we extract from our fit to the quasi-elastic widths are quite different than obtained in the previous low-resolution studies. Fu *et al.* extracted a single value for the characteristic jump length of $\ell_0 = 1.2 \pm 0.4$ Å. The value we extract from our fit at 50 K 4.0 ± 1.5 Å. Likewise, Fu *et al.* found a residence time at 50 K of 4.5 ps while we find 11.1 ps. As stated earlier, it is not possible to see the same range of dynamics with the HFBS instrument as was seen by Fu *et al.* Even so, it is possible that we are seeing the low frequency dynamics of the same process, which would explain the correlation of diffusion coefficients in spite of differences in residence times and jump lengths.

5. CONCLUSIONS

In conclusion, we observe no diffusive motion below 30 K. Certainly, we see no diffusion characteristic of a traditional liquid phase within the

pore. We do observe a slow diffusive motion, characterized by a fixed length diffusion model, between 30 and 40 K. This motion is consistent with hopping between absorption sites within the zeolite pore. Above 40 K the simple fixed jump length model no longer provides an adequate physical description of the results. However, the variable jump length model employed in previous measurements does provide a reasonable description of the results and the extracted diffusion constant agrees well with the previous measurements.

These studies show that the hydrogen molecules in the zeolite at low coverage are strongly localized to specific absorption sites in the zeolite framework. This is evident from the site-to-site hopping and the low diffusion observed in this measurement. It is very unlikely that sufficient overlap of the hydrogen wavefunction would occur to allow Bose condensation. This is consistent with the conclusions reached in the structural studies of Fang *et al.*[16] Furthermore, Fang's results at fillings up to full pore suggest that the hydrogen in the zeolite is always strongly localized to specific absorption sites. The two sites, s1 and s2, identified by Fang *et al.* account for all hydrogen in the pores. At any temperature where Bose condensation could be expected to occur these studies show that the hydrogen is strongly localized to specific sites. These studies and the quasi-elastic scattering studies of Fu *et al.*[17] support this interpretation. Thus, it is unlikely that zeolites, such as 13X, will be successful as a host for the observation of Bose condensation in hydrogen.

ACKNOWLEDGMENTS

We would like to acknowledge Mr. David Narehood for help with the collection of the experimental data and Dr. Brian Toby and Dr. Dan Neumann for useful discussions. This work was supported by the National Science Foundation under Grant DMR 9970126.

REFERENCES

1. J. Wilks and D. S. Betts, in *An Introduction to Liquid Helium*, Clarendon Press, Oxford (1987).
2. M. H. Anderson *et al.*, *Science* **269**, 198 (1995).
3. V. L. Ginzburg and A. A. Sobyanin, *Sov. Phys. JETP Lett.* **15**, 242 (1972).
4. H. J. Maris, G. M. Seidel, and T. E. Huber, *J. Low Temp. Phys.* **51**, 471 (1983).
5. G. M. Seidel, H. J. Maris, F. I. B. Williams, and J. G. Gordon, *Phys. Rev. Lett.* **56**, 2380 (1986).
6. I. F. Silvera, *Rev. Mod. Phys.* **52**, 393 (1980).
7. M. Bretz and A. L. Thompson, *Phys. Rev. B* **24**, 467 (1981).
8. M. Rall, J. P. Brison, and N. S. Sullivan, *Phys. Rev. B* **44**, 9639 (1991).
9. H. K. Christenson, *J. Phys. Cond. Matter* **13**, R95–R133 (2001).

10. J. L. Tell and H. J. Maris, *Phys. Rev. B* **28**, 5122 (1983).
11. R. H. Torii, H. J. Maris, and G. M. Seidel, *Phys. Rev. B* **41**, 7167 (1990).
12. H. J. Maris, G. M. Seidel, and F. I. B. Williams, *Phys. Rev. B* **36**, 6799 (1987).
13. N. S. Sullivan, M. Rall, and J. P. Brisson, *J. Low Temp. Phys.* **98**, 383 (1995).
14. Y. Sonnenblick, E. Alexander, Z. H. Kalman, and I. T. Steinberger, *Chem. Phys. Lett.* **52**, 276 (1977).
15. Grade 13X from Union Carbide Corporation, Box 372, South Planfield, New Jersey 07080.
16. M. Fang, Y. Wang, and P. E. Sokol, *Phys. Rev. B* **50**, 12291 (1994).
17. H. Fu, F. R. Trouw, and P. E. Sokol, *J. Low Temp. Phys.* **116**, 149 (1999).
18. P. M. Gehring and D. A. Neumann, *Physica B* **64**, 241 (1998).
19. D. H. Olson, *J. Phys. Chem.* **74**, 2758 (1970).
20. M. Rall, J. P. Brison, and N. S. Sullivan, *Phys. Rev. B* **44**, 9932 (1991).
21. C. T. Chudley and R. J. Elliot, *Proc. Phys. Soc.* **77**, (1961).
22. A. Furrer, in *Neutron Scattering from Hydrogen in Materials*, World Scientific (1994).
23. P. A. Egelstaff, in *An introduction to the Liquid State*, Academic Press (1967).
24. H. M. Rietveld, *Acta Cryst.* **22**, 151 (1967).
25. H. M. Rietveld, *J. Appl. Cryst.* **Z**, 65 (1969).
26. J. D. Jorgensen and F. J. Rotella, *J. Appl. Crystallogr.* **15**, 27 (1982).
27. R. B. VonDreele, J. D. Jorgensen, and C. E. Windsor, *J. Appl. Crystallogr.* **15**, 581 (1982).
28. M. P. Fang, P. E. Sokol, and Y. Wang, *Phys. Rev. B* **50**; **17**, 12291 (1994).
29. GSAS, © 1985–1994, The regents of the University of California.